Oct 14th, 12:00 AM

Buckling Studies of Thin-walled Channel Sections under Combined Bending and Shear

Cao Hung Pham

Gregory J. Hancock

Nineteenth International Specialty Conference on Cold-Formed Steel Structures
St. Louis, Missouri, U.S.A, October 14 & 15 2008

Buckling Studies of Thin-Walled Channel Sections under Combined Bending and Shear

Cao Hung Pham[1] and Gregory J. Hancock[2]

Abstract

Thin-walled section members can be subjected to axial force, bending and shear. In the cases of cantilever beams and continuous lapped purlins, where combined bending and shear occur at the purlin section just outside the end of the lap, thin-walled sections may buckle at a lower stress than if only one action was present without the other. The computational modelling of the thin-walled steel sections is implemented by means of a spline finite strip analysis to determine the elastic buckling stresses of channel sections subject to bending and shear alone and interaction relations under combined bending and shear. Both unlipped and lipped channels are studied where the main variables are the flange width, different boundary conditions and shear flow distribution. Comparisons between cases, and with classical solutions are included in this report.

1. Introduction

The elastic critical stress for local buckling of flat rectangular plates has been extensively investigated and summarised by many investigators (Timoshenko and Gere, 1961; Bulson, 1970; Bleich, 1952, Allen and Bulson, 1980). For a thin flat plate simply supported along all four edges, the buckling stress of an elastic rectangular plate for local buckling in compression, bending or shear is given by Timoshenko and Gere (1961) as:

$$f_{ol} = k\frac{\pi^2 E}{12(1-\nu^2)}\left(\frac{t}{b_1}\right)^2 \qquad (1)$$

[1] Doctoral Candidate, School of Civil Engineering, The University of Sydney, Sydney NSW 2006, Australia.
[2] Bluescope Steel Professor of Steel Structures and Dean of Engineering and Information Technologies, The University of Sydney, Sydney NSW 2006, Australia.

where E = modulus of elasticity; ν = Poisson's ratio; b_1 = width of the plate; t = thickness of the plate; a = length of the plate. k is the plate local buckling coefficient, which depends on the boundary conditions and the aspect ratio of the rectangular plate a/b_1.

For plates with all edges simply supported subjected to pure bending: $k = 23.9$

For plates with all edges simply supported subjected to pure shear: $k = 5.34 + \frac{4}{(a/b_1)^2}$. As the plate is shortened, the number of local buckles is reduced and the value of k for a plate simply supported on all four edges is increased from 5.34 for a very long plate to 9.34 for a square plate.

The traditional approach has been to investigate shear plate buckling in the web alone and to ignore the behaviour of the whole section including the flanges. There does not appear to have been any consistent investigations of the full section buckling of thin-walled sections under shear until recently Pham and Hancock (2007) provided solutions to the shear buckling of complete channel sections loaded in pure shear parallel with the web by using spline finite strip analysis (Lau and Hancock, 1986). The analysis results show that the flanges can have a significant influence on improvement of the shear buckling capacity of thin-walled channel sections. Further, it was also demonstrated that the lack of lateral restraint for sections with narrow flanges can lead to premature buckling of the section in a twisting and lateral buckling mode.

When high bending and high shear act simultaneously, the combination of shear stress and bending stress produces a further reduction in the capacity of the web. The interaction equation is a circular formula as shown in Fig 1. This interation equation is based upon an approximation to the theoretical interaction of local buckling resulting from shear and bending as derived by Timoshenko and Gere (1961). Fig 1 shows the interaction between f_b/f_{cr} and τ/τ_{cr} in which f_b is the actual computed bending stress, f_{cr} is the theoretical buckling stress in pure bending, τ is the actual computed shear stress, and τ_{cr} is the theoretical buckling stress in pure shear. The relationship between f_b/f_{cr} and τ/τ_{cr} can be approximated by the following equation which is a part of the unit circle:

$$\left(\frac{f_b}{f_{cr}}\right)^2 + \left(\frac{\tau}{\tau_{cr}}\right)^2 = 1 \qquad (2)$$

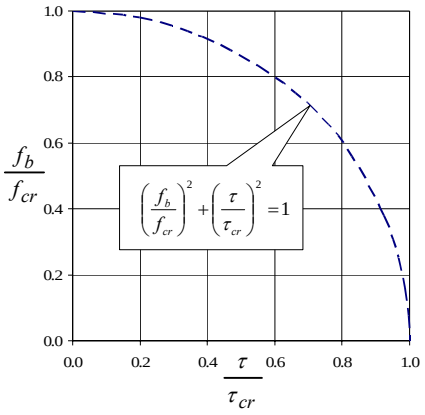

Figure 1. Interaction relation between f_b/f_{cr} and τ/τ_{cr} in a rectangular plate

To analyse complete channel sections under combined bending and shear, the buckling analysis is based on a spline finite strip analysis (Lau and Hancock, 1986) implemented by Gabriel Eccher in the program ISFSM Isoparametric Spline Finite Strip Method (Eccher, 2007). Both unlipped and lipped channels of varying section geometry are investigated. Three different methods, which represent different ways of incorporating the shear stresses in the thin-walled section, are used in this paper. These include pure shear in the web only, pure shear in the web and the flanges, and a shear distribution similar to that which occurs in practice allowing for section shear flow. Each method of the shear stress distributed is combined with pure bending to produce the interaction relation. A significant outcome of the study is lateral buckling under shear of sections with narrow flanges.

2. Modelling Sections under Combined Bending and Shear

2.1 Spline Finite Strip Method

The spline finite strip method is a development of the semi-analytical finite strip method originally derived by Cheung (1976). It uses spline functions in the longitudinal direction in place of the single half sine wave over the length of the section, and has been proven to be an efficient tool for analysing structures with constant geometric properties in a particular direction, generally the longitudinal one. The advantage of the spline finite strip analysis is that it allows more complex types of loading and boundary conditions other than simple supports to be easily investigated and buckling in shear is also easily accounted for. Initially, the spline finite strip method was fully developed for the linear elastic structural analysis of folded plate structures by Fan and Chueng (1982). The spline finite strip method was then extended to buckling and nonlinear analyses

of flat plates and folded-plate structures by Hancock *et al.* (1986, 1989 and 1991). The spline finite strip method involves subdividing a thin-walled member into longitudinal strips where each strip is assumed to be free to deform both in its plane (membrane displacements) and out of its plane (flexural displacements). The ends of the section under study are free to deform longitudinally but are prevented from deforming in a cross-sectional plane.

Unlipped Channel

The geometry of the unlipped channel studied is shown in Fig 2. The channel sections consist of a web of width 200 mm, a flange of width 0.01 mm to 160 mm, both with thickness of 2 mm. The member is subdivided into 36 longitudinal strips which include 16 strips in the web and 10 strips in each flange. The length of the member studied is 1000 mm. The aspect ratio of the web rectangular plate is therefore $a/b_1 = 5$.

Lipped Channel

The geometry of the lipped channel studied is shown in Fig 3. The channel section consists of a web of width 200 mm, a flange of width 0.01 mm to 160 mm, a lip size of 20 mm, all with thickness 2 mm. The member is subdivided into 40 longitudinal strips which include 16 strips in the web, 10 strips in each flange and 2 strips in each lip. The length of the member studied is 1000 mm. The aspect ratio of the web rectangular plate is therefore $a/b_1 = 5$.

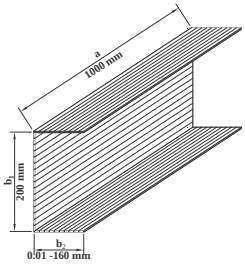

Figure 2. Unlipped Channel Geometry

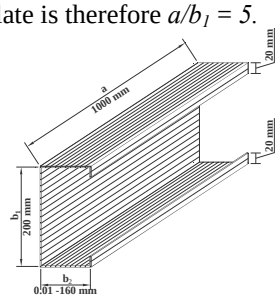

Figure 3. Lipped Channel Geometry

2.2 Shear Stress Distribution and Pure Bending

In order to demonstrate the different ways in which a channel member may buckle under shear stress, four cases of shear stress distribution are investigated. In *Cases A* and *B*, uniform pure shear stress is applied throughout the web panel as shown in Fig 4(a), 5(a). The only difference between *Case A* and *B* is that two longitudinal edges of the channel member in *Case A* are restrained laterally

whereas there is no restraint along the two longitudinal edges in *Case B*. In *Case C*, the pure shear stress is uniform in both the web and the flanges as shown in Fig 4(b), 5(b). Although this case is unrealistic in practice, it investigates the effect of the flanges on the buckling of the member under pure shear stress. *Case D* models the case which occurs in practice namely, a shear flow distribution as shown in Fig 4(c), 5(c) resulting from a shear force parallel with the web. To simulate the variation in shear stress, each strip in the cross-section is assumed to be subjected to a pure shear stress which varies from one strip to the other strip. The more the cross-section is subdivided into strips, the more accurately the shear stress is represented in order to match the practical shear flow distribution. Each above case is also subjected to pure bending which is shown in the following figures:

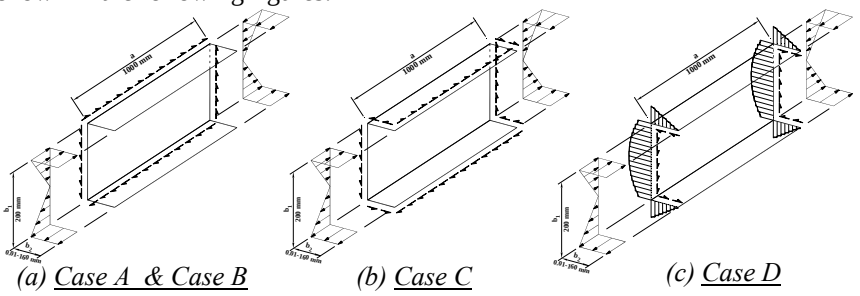

(a) Case A & Case B *(b) Case C* *(c) Case D*

Figure 4. Stress Distribution in Unlipped Channel

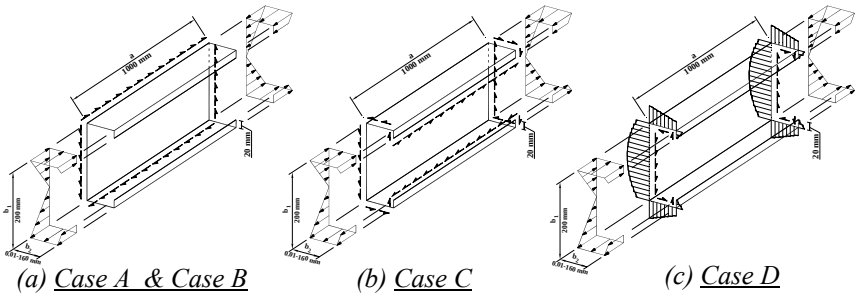

(a) Case A & Case B *(b) Case C* *(c) Case D*

Figure 5. Stress Distribution in Lipped Channel

2.3 Lateral Restraints and Boundary Conditions

Two types of boundary conditions are used for the analysis of all cases in this report. A combination of lateral restraints along the two longitudinal edges of web panels and simply supported edges of the end cross-section plane is applied in *Case A*. In the remaining cases *(Cases B,C & D)*, there are no lateral restraints along the two longitudinal edges of web panels. All edges of the end cross-

section are simply supported. Fig 6 and Table 1 show the lateral restraints and boundary conditions of the unlipped channel. Fig 7 and Table 2 show those for the lipped channel.

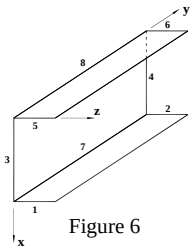

Figure 6

Cases	Edges	*u*	*v*	*w*
A	1 2 5 6	1	0	0
	3 4 7 8	0	0	1
B,C & D	1 2 5 6	1	0	0
	3 4	0	0	1
	7 8	0	0	0
Note: *u, v* and *w* are translations in the *x,y* and *z* directions respectively. 0 denotes free and 1 denotes restraint DOF				

Table 1. Boundary Conditions of Unlipped Channel

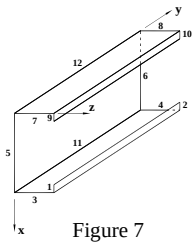

Figure 7

Cases	Edges	*u*	*v*	*w*
A	3 4 7 8	1	0	0
	1 2 5 6 9 10 11 12	0	0	1
B,C & D	3 4 7 8	1	0	0
	1 2 5 6 9 10	0	0	1
	11 12	0	0	0
Note: *u, v* and *w* are translations in the *x,y* and *z* directions respectively. 0 denotes free and 1 denotes restraint DOF				

Table 2. Boundary Conditions of Lipped Channel

3. Results of Buckling Analyses

3.1 Unlipped Channel Section – Length = 1000 mm, $a/b_1 = 5.0$, *Case A*

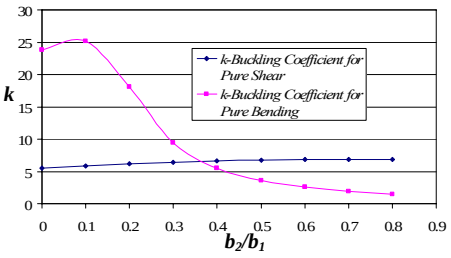

Figure 8. The Ratio of Flange and Web Widths (b_2/b_1) and The Buckling Coefficients (k) of Unlipped Channel Section for *Case A*

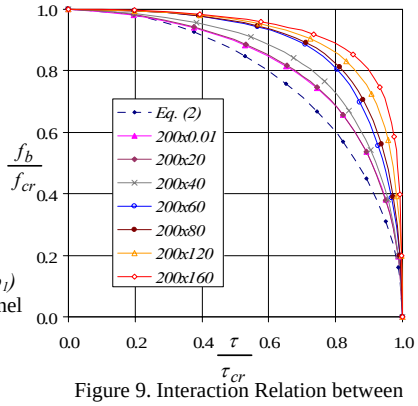

Figure 9. Interaction Relation between f_b/f_{cr} and τ/τ_{cr} for *Case A*

The results of the bucking analyses of the unlipped channel section for *Case A* with a length of 1000 mm and lateral restraints along the two longitudinal edges of web panel are shown in Fig 8 for the ratios of flange to web widths (b_2/b_1)

from 0.00005 to 0.8. The buckling coefficient curve *(k)* of the unlipped channel section subjected to pure shear is shown as the square line ( ), whereas the diamond line ( ) represents the coefficient curve *(k)* for pure bending. For pure shear, when the flange width is very small (0.01 mm), the value of *k* is 5.51 which is very close to the theoretical result (Timoshenko and Gere, 1961; Bulson, 1970; Bleich, 1952; Allen and Bulson, 1980). As the flange width increases to 160 mm, the value of *k* increases to 6.905 as a result of the elastic torsional restraint of the flange on the web. For pure bending, the buckling coefficient *(k)* is 23.79 when the ratio of b_2/b_1 is 0.00005. This value of *k* is close to the theoretical result of 23.9 (Timoshenko and Gere, 1961; Bulson, 1970; Bleich, 1952; Allen and Bulson, 1980). As the ratio of b_2/b_1 increases to 0.1, the value of *k* improves to 25.14. The explanation for this fact is that the presence of small flange contributes to buckling capacity of channel section subjected to pure bending. The buckling mode occurs mainly in the web. However, when the ratio of b_2/b_1 increases from 0.1 to 0.8, the value of *k* reduces dramatically due to uniform compression stress in wider flange which causes the buckling mode to occur mainly in the flange.

Fig 9 shows the interaction relation curves between f_b/f_{cr} and τ/τ_{cr} for *Case A* with lateral restraints along the two longitudinal edges of web panel for different flange widths. The corresponding buckling mode shapes for *Case A* under combined bending and shear are shown in Fig 10.

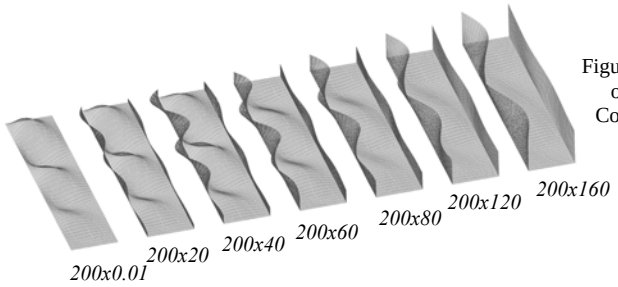

Figure 10. Buckling Mode Shape of Unlipped Section under Combined Bending and Shear for *Case A*

3.2 Unlipped Channel Section – Length = 1000 mm, a/b_1 = 5.0, *Case B*

Fig 11 shows the results for the buckling analyses of the unlipped channel section for *Case B* with a length of 1000 mm and the ratios of flange to web width *(b_2/b_1)* from 0.00005 to 0.8. In this case, there are no lateral restraints along the two longitudinal edges of web panel.

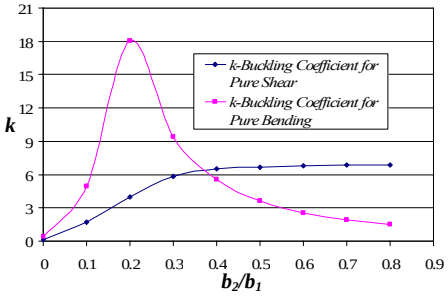

Figure 11. The Ratio of Flange and Web Widths (b_2/b_1) And The Buckling Coefficients (k) of Unlipped Channel Section for *Case B*

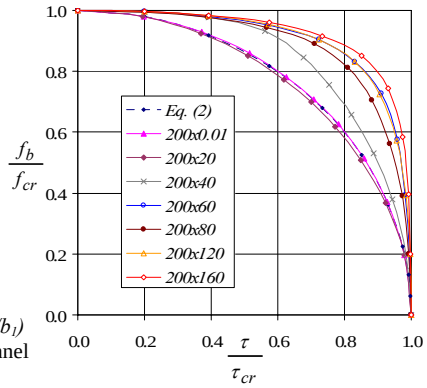

Figure 12. Interaction relation between f_b/f_{cr} and τ/τ_{cr} for *Case B*

The buckling coefficient curve (k) of the unlipped channel section subjected to pure shear is shown as the square line (—◆—), whereas the diamond line (—■—) represents the buckling coefficient curve (k) for pure bending. For pure shear, when the ratio of flange to web width (b_2/b_1) is 0.00005, the value of k is very close to zero (0.109). The channel member buckles sideways as demonstrated previously (Pham and Hancock, 2007). It is interesting to note that when the ratio of b_2/b_1 increases to around 0.3, the value of k_v increases dramatically to 5.853. The buckling mode shape is shown in the analysis of Pham and Hancock (2007) as a twisting mode. As the ratio of b_2/b_1 keeps increasing to 0.8, the value of k_v improves to 6.889. The explanation is due to the fact that there is apparently more lateral and torsional restraint being provided by the flanges. For pure bending, the buckling coefficient (k) is 0.436, when the ratio of b_2/b_1 is 0.00005. For *Case B* with no lateral restraint along the two longitudinal edges of web panel, the channel member also buckles sideways. As the ratio of b_2/b_1 increases to 0.2, the value of k increases dramatically to 18.064. This can be explained by the fact that the flanges minimise sideways buckling of the section although the buckling coefficient does not reach 23.9 as for a laterally restrained section. However, it should be noted that when the ratio of b_2/b_1 increases further from 0.2 to 0.8, the value of k reduces dramatically from 18.064 to 1.482 due to the uniform compression in wider flange which results in the buckling mode being mainly in the flange.

Fig 12 shows the interaction relation curves for different flange widths between f_b/f_{cr} and τ/τ_{cr} for *Case B* with no lateral restraint along the two longitudinal edges of web panel. The corresponding buckling mode shapes for *Case B* under combined bending and shear are shown in Fig 13.

As can be seen in Fig 12, when the flange width is very small (0.01mm – 20 mm), the interaction relation curves lie slightly below the circular curve. The interaction between bending and shear is therefore significant due to the fact that the small flange width causes twisting buckling mode as shown in Fig 13. As the flange width increases, the interaction relation curves lie further above the circular curve. The interaction relation is therefore less significant. The explanation is quite similar to that of *Case A* described above. As can be seen in Fig 13, the buckling mode occurs mainly in the web due to uniform compression stress and no shear stress distribution in wider flange.

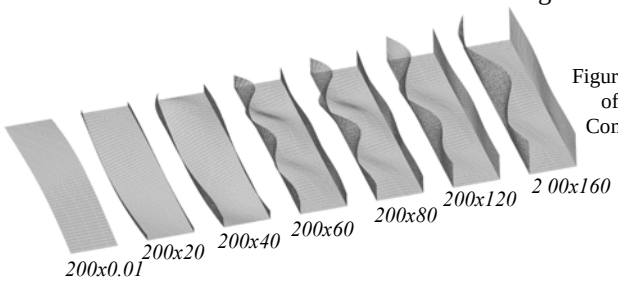

Figure 13. Buckling Mode Shape of Unlipped Section under Combined Bending and Shear for *Case B*

3.3 Unlipped Channel Section – Length = 1000 mm, a/b_1 = 5.0, *Case C*

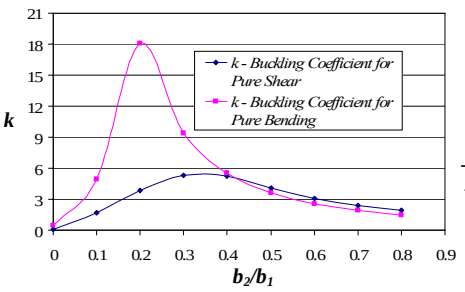

Figure 14. The Ratio of Flange and Web Widths (b_2/b_1) and The Buckling Coefficients (k) of Unlipped Channel Section for *Case C*

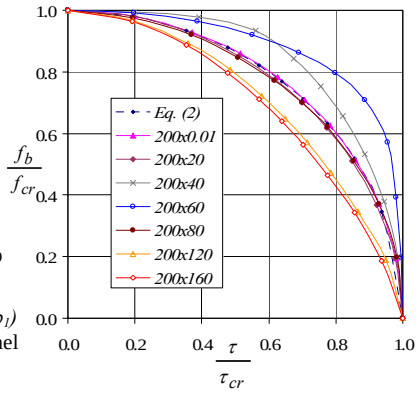

Figure 15. Interaction relation between f_b/f_{cr} and τ/τ_{cr} for *Case C*

The results of the bucking analyses of the unlipped channel section for *Case C* with a length of 1000 mm and pure shear flow applied in the web and the flanges are shown in Fig 14 for the ratios of flange to web widths (b_2/b_1) from 0.00005 to 0.8. The boundary conditions are the same as those of *Case B*. The square line (—◆—) and the diamond line (—■—) represent the coefficient curves (k) for pure shear and pure bending respectively. For pure shear, when the ratio of flange to web width (b_2/b_1) increases from 0.00005 to 0.3, the value of k is not

significantly different from that of *Case B.* However, from the ratio of b_2/b_1 of 0.4 the value of *k* for *Case C* reduces dramatically. The explanation is mainly a result of the effect of shear stresses in the flanges. For pure bending, the buckling coefficient curve *(k)* is identical to that of *Case B* as the bending stress distribution is the same.

Fig 15 shows the interaction relation curves between f_b/f_{cr} and τ/τ_{cr} for different flange widths for *Case C* where pure shear flow is applied in both the web and the flanges. The corresponding buckling mode shapes for *Case C* under combined bending and shear are shown in Fig 16.

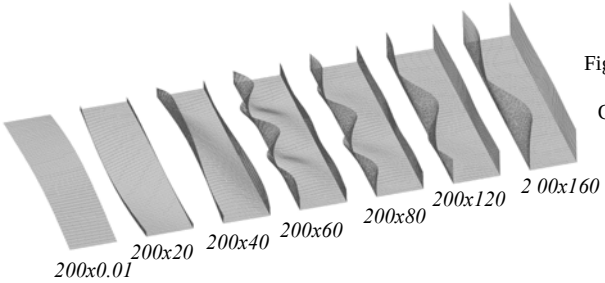

Figure 16. Buckling Mode Shape of Unlipped Section under Combined Bending and Shear for *Case C*

It can be seen in Fig 16 that when the flange width is very small (0.01mm – 20 mm), the interaction relation curves lie slightly below the circular curve as for *Case B*. The interaction is significant as the twisting buckling mode is the main reason for the interaction. As the ratio of b_2/b_1 increases from 0.2 to 0.3, the relation curves make above the circular curve. The interaction relation is then less significant. However, it is interesting to note that the interaction curve is slightly below the circular curve at the ratio of b_2/b_1 of 0.4. As the ratio of b_2/b_1 increases to 0.8, the interaction relation curves lie further below the circular curve so that the interaction between bending and shear is very significant. The explanation for this fact is mainly due to interaction of shear buckling and compression in the flange.

3.4 Unlipped Channel Section – Length = 1000 mm, a/b_1 = 5.0, *Case D*

Fig 17 shows the results for the buckling analyses of the unlipped channel section for *Case D* with a length of 1000 mm and the ratios of flange to web width (b_2/b_1) from 0.00005 to 0.8. The boundary conditions are the same as those of *Case B.* The square line (—◆—) and the diamond line (—■—) represent the coefficient curves *(k)* for pure shear and pure bending respectively. For pure shear, the buckling coefficient curve *(k)* is quite similar to that of *Case B* although the value of *k* is slightly lower due to the effect of the shear stress gradient in the flanges and the parabolic shear stress distribution in the web. For

pure bending, the buckling coefficient curve *(k)* is identical to that of *Case B* as the bending stress distribution is the same.

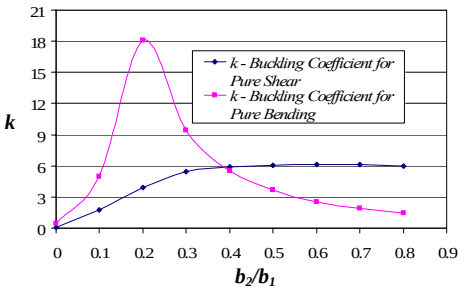

Figure 17. The Ratio of Flange and Web Widths (b_2/b_1) and The Buckling Coefficients *(k)*Of Unlipped Channel Section for *Case D*

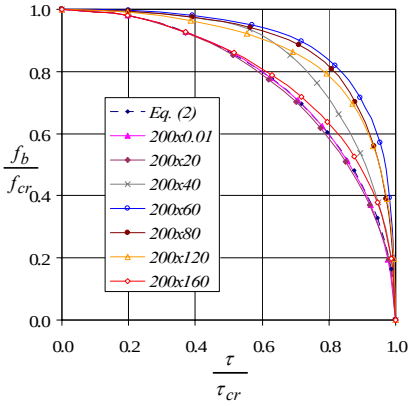

Figure 18. Interaction relation between f_b/f_{cr} and τ/τ_{cr} for *Case D*

Fig 18 shows the interaction relation curves between f_b/f_{cr} and τ/τ_{cr} for the different flange widths for *Case D.* The corresponding buckling mode shapes for *Case D* under combined bending and shear are shown in Fig 19.

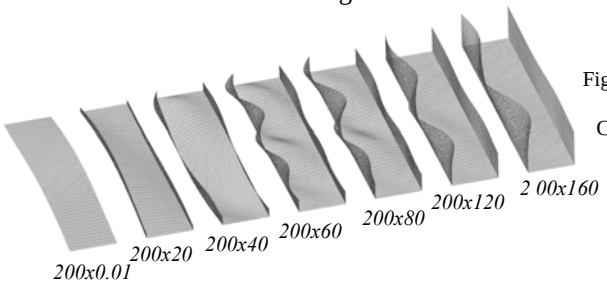

Figure 19. Buckling Mode Shape of Unlipped Section under Combined Bending and Shear for *Case D*

As can be seen in Fig 18, when the flange width is very small (0.01mm – 20 mm), the interaction relation curves are similar to those of *Cases B & C* described above. The interaction between bending and shear is significant due to the twisting buckling mode shown in Fig 19. As the ratio of b_2/b_1 increases to 0.3, the interaction relation curves lie further above the circular curve. The interaction is therefore less significant. It can be noted that when the ratio of b_2/b_1 increases further from 0.3 to 0.8, the interaction relation curve gets closer to the circular curve so that the interaction becomes more significant. The explanation for this fact is due to the presence of both the uniform compression stress and the actual shear stress distribution in the wider flange.

3.5 Lipped Channel Section – Length = 1000 mm, $a/b_1 = 5.0$, *Case A*

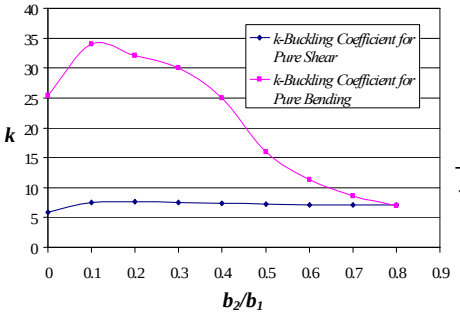

Figure 20. The Ratio of Flange and Web Widths (b_2/b_1) and The Buckling Coefficients (k) of Lipped Channel Section for *Case A*

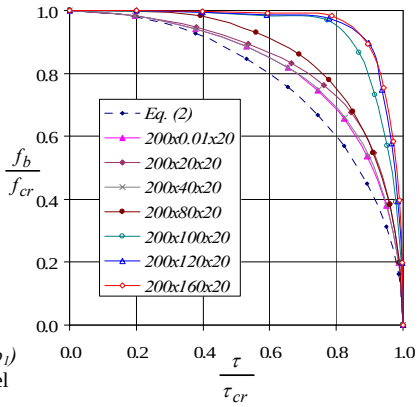

Figure 21. Interaction relation between f_b/f_{cr} and τ/τ_{cr} for *Case A*

The results of the bucking analyses of the lipped channel section for *Case A* with a length of 1000 mm are shown in Fig 20 for the ratios of flange to web widths (b_2/b_1) from 0.00005 to 0.8. In this case, there are lateral restraints along the two longitudinal edges of web panel. The lip size of 20 mm is used throughout the analyses. The buckling coefficient curve (k) of the lipped channel section subjected to pure shear is shown as the square line (—◆—), whereas the diamond line (—■—) represents the coefficient curve (k) of pure bending. For pure shear, when the flange width is very small (0.01 mm), the value of k is 5.885 which is slightly greater than that of *Case A* for the unliped channel due to the presence of the two lips which improve the shear capacity of the channel section member. As the ratio of b_2/b_1 increases to 0.1, the value of k goes up rapidly. The explanation is that the small flange width with the lip contributes significantly to the shear buckling capacity of the lipped channel section. It should be noted that when the ratio of b_2/b_1 increases from 0.1 to 0.2, the value of k improves slowly from 7.561 to 7.691 respectively and then reduces to 7.073 as the ratio of b_2/b_1 increases to 0.8. The explanation for this fact is due to the effect of flange slenderness. As the flange width is small, there is little or no effect of flange slenderness on the shear buckling capacity. However, when flange width increases, the effect of flange slenderness is quite considerable. For pure bending, the buckling coefficient (k) is 25.42 when the ratio of b_2/b_1 is 0.00005. This value of k is slightly greater than to the theoretical result of 23.9 (Timoshenko and Gere, 1961; Bulson, 1970; Bleich, 1952; Allen and Bulson, 1980). As the ratio of b_2/b_1 increases to 0.1, the value of k improves to 34.01. The explanation for this fact is that the presence of small flanges and lips

contribute to the buckling capacity of the channel section subjected to pure bending so that the buckling mode occurs mainly in the web. However, when the ratio of b_2/b_1 increases from 0.1 to 0.3, the value of k reduces slightly to 25.04 due to the uniform compression stress in the wider flange. The mode of buckling is mainly local buckling mode in the flange. It is interesting to note that when the ratio of b_2/b_1 increases further from 0.4 to 0.5, the value of k drops significantly from 25.04 to15.98. The reason is that the member buckles in the distortional mode with the wider flange width. The value of k then reduces slightly to 6.94 as the ratio of b_2/b_1 increases to 0.8. The buckling mode is mainly distortional buckling mode for wide flanges.

Fig 21 shows the interaction relation curves between f_b/f_{cr} and τ/τ_{cr} for different flange widths for *Case A* with lateral restraint along the two longitudinal edges of the web panel. The corresponding buckling mode shapes for *Case A* in the critical case of combined bending and shear are shown in Fig 22.

Figure 22. Buckling Mode Shape of Lipped Section under Combined Bending and Shear for *Case A*

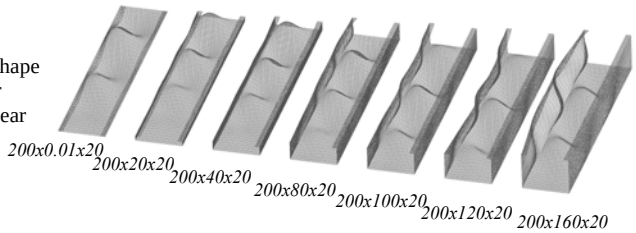

As can be seen in Fig 21, when the flange width is in the range from 0.01mm – 80 mm, the interaction relation curves lie slightly above the circular curve. This shows that the interaction relation under combined bending and shear is significant. As the flange width increases from 80 mm to 160 mm, the interaction relation curves lie further above circular curve. The interaction is therefore not significant. This can be explained for *Case A* where there is no shear stress distribution in the flange, so that the uniform compression stress in the wider flange mainly causes distortional buckling as shown in Fig 22.

3.6 Lipped Channel Section – Length = 1000 mm, a/b_1 = 5.0, *Case B*

Fig 23 shows the results of the buckling analyses of the lipped channel section for *Case B* with a length of 1000 mm and the ratios of flange to web width (b_2/b_1) from 0.00005 to 0.8. In this case, there are no lateral restraints along the two longitudinal edges of web panel. The lip size of 20 mm is used throughout the analyses. The buckling coefficient curve *(k)* of the lipped channel section subjected to pure shear is shown as the square line (—◆—), whereas the diamond line (—■—) represents the coefficient curve *(k)* for pure bending.

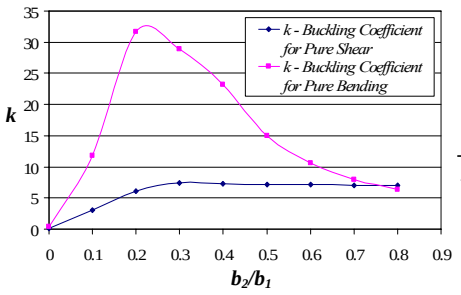

Figure 23. The Ratio of Flange and Web Widths *(b₂/b₁)* and The Buckling Coefficients *(k)o* f Lipped Channel Section for *Case B*

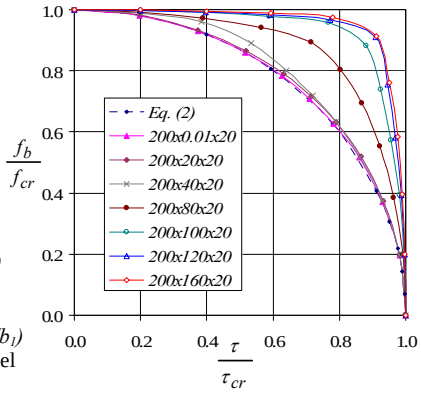

Figure 24. Interaction relation between f_b/f_{cr} and τ/τ_{cr} for *Case B*

For pure shear, when the ratio of flange to web width *(b₂/b₁)* is 0.00005, the value of *k* is then very close to zero (0.131). The channel member buckles sideways (Pham and Hancock, 2007). It is interesting to note that when the ratio of b_2/b_1 increases to 0.3, the value of *k* increases dramatically to 7.376. With a very small flange width, the buckling mode shown in the analyses of Pham and Hancock (2007) is twisting mode. As the ratio of b_2/b_1 keeps increasing to 0.8, the value of *k* improves and get closer to that of *Case A* for the unlipped channel described above. The reason for this fact is that the flanges with lips are long enough to give full lateral restraint to the lipped channel section members. For pure bending, the buckling coefficient *(k)* is 0.349, when the ratio of b_2/b_1 is 0.00005. For *Case B* with no lateral restraint along the two longitudinal edges of web panel, the channel member also buckles sideways. As the ratio of b_2/b_1 increases to 0.2, the value of *k* increases dramatically to 31.71. This can be explained by the fact that the flanges with lips contribute significantly to the buckling capacity of the channel section subjected to pure bending. However, it should be noted that when the ratio of b_2/b_1 increases further from 0.2 to 0.4, the value of *k* reduces from 31.71 to 23.17 due to uniform compression in wider flange. The buckling mode is mainly local buckling. As the ratio of b_2/b_1 increases from 0.4 to 0.8, the value of *k* drops dramatically from 23.17 to 6.42. The mode of buckling is the distortional buckling due to the uniform compression stress in wider flange.

Fig 24 shows the interaction relation curves between f_b/f_{cr} and τ/τ_{cr} for different flange widths for *Case B* with no lateral restraint along the two longitudinal edges of web panel. The corresponding buckling mode shapes for *Case B* under combined bending and shear are shown in Fig 25.

As can be seen in Fig 24, when the flange width is very small (0.01mm – 40 mm), the interaction relation curves lie very close to the circular curve. The interaction between bending and shear is significant. The reason for this is due to the fact that the small flange width allows the twisting buckling mode as shown in Fig 25. As the flange width increases , the interaction relation curves lie above the circular curve. The interaction relation is therefore less significant. Also can be seen in Fig 25, when the ratio of b_2/b_1 increases further from 0.5 to 0.8, the interaction relation curves are further above circular curve. The interaction is therefore not significant. The explanation is similar to that for *Case A.* No shear stress in the flange and a uniform compression stress in wider flange mainly cause distortional buckling as shown in Fig 25.

Figure 25. Buckling Mode Shape of Lipped Section under Combined Bending and Shear for *Case B*

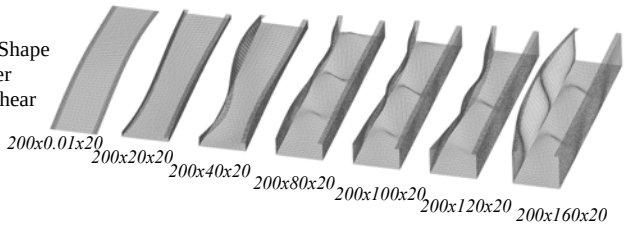

3.7 Lipped Channel Section – Length = 1000 mm, a/b_1 = 5.0, *Case C*

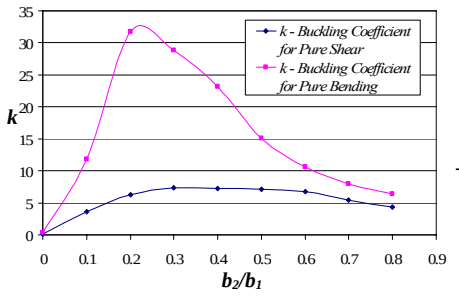

Figure 26. The Ratio of Flange and Web Widths (b_2/b_1) and The Buckling Coefficients (k) of Lipped Channel Section for *Case C*

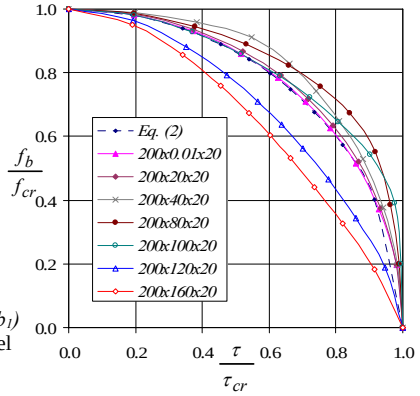

Figure 27. Interaction relation between f_b/f_{cr} and τ/τ_{cr} for *Case C*

The results of the bucking analyses of the lipped channel section for *Case C* with a length of 1000 mm are shown in Fig 26 for the ratios of flange to web widths (b_2/b_1) from 0.00005 to 0.8. The boundary conditions are the same as those of *Case B.* The lip size of 20 mm is used throughout the analyses. The square line (—◆—) and the diamond line(—■—) represent the coefficient curves (k) for pure shear and pure bending respectively. For pure shear, when the ratio

of the flange to web width (b_2/b_1) increases from 0.00005 to 0.3, the value of k is not significantly different from that of *Case B.* However, when the ratio of b_2/b_1 increases further from 0.4 to 0.8, the value of k for *Case C* reduces dramatically from 7.337 to 4.37. The explanation is mainly a result of the effect of shear stresses in the flanges. For pure bending, the buckling coefficient curve *(k)* is identical to that of *Case B* as the bending stress distribution is the same.

Fig 27 shows the interaction relation curves between f_b/f_{cr} and τ/τ_{cr} for different flange widths for *Case C* where pure shear flow is applied in both web, flanges and lips. The corresponding buckling mode shapes for *Case C* under combined bending and shear are shown in Fig 28.

Figure 28. Buckling Mode Shape of Lipped Section under Combined Bending and Shear for *Case C*

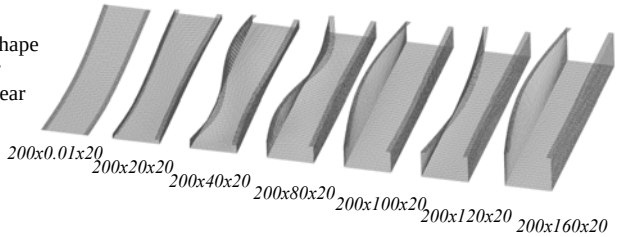

It can be seen in Fig 27 that when the flange width is in the range from 0.01mm – 100 mm, the interaction relation curves lie slightly above the circular curve. The interaction is therefore significant. The explanation is mainly due to the twisting buckling mode when the flange width is small. As the ratio of b_2/b_1 increases further from 0.6 to 0.8, the relation curves make below the circular curve. This shows that the interaction between bending and shear is very significant. The explanation for this fact is mainly due to the interaction of pure shear stress and uniform compression stress in the flange. As can be seen in Fig 28, the buckling mode is the twisting of the flange distortional buckling under shear and compression. There is little or no buckling in the web.

3.8 Lipped Channel Section – Length = 1000 mm, $a/b_1 = 5.0$, *Case D*

Fig 29 shows the results of the buckling analyses of the lipped channel section for *Case D* with a length of 1000 mm and the ratios of flange to web width (b_2/b_1) from 0.00005 to 0.8. The boundary conditions are the same as those of *Case B.* The square line ( ) and the diamond line ( ) represent the coefficient curves *(k)* for pure shear and pure bending respectively. For pure shear, the buckling coefficient curve *(k)* is quite similar to that of *Case B.* The value of k is slightly lower due to the effect of the shear stress gradient in the flange and the parabolic shear stress distribution in the web. For pure bending, the buckling coefficient curve *(k)* is identical to that of *Case B* as the bending stress distribution is the same.

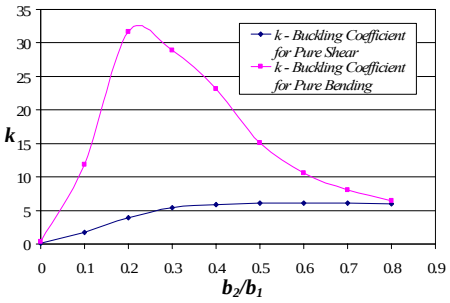

Figure 29. The Ratio of Flange and Web Widths *(b_2/b_1)* and The Buckling Coefficients *(k)* of Lipped Channel Section for *Case D*

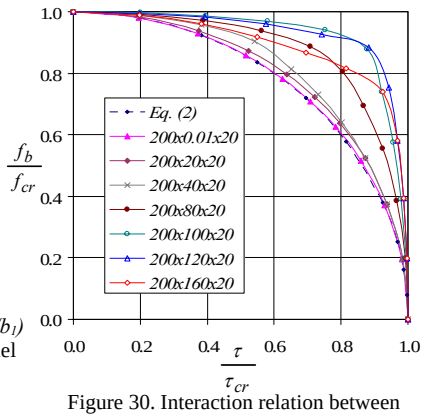

Figure 30. Interaction relation between f_b/f_{cr} and τ/τ_{cr} for *Case D*

Fig 30 shows the interaction relation curves between f_b/f_{cr} and τ/τ_{cr} for different flange widths for *Case D* where actual shear flow is applied. The corresponding buckling mode shapes for *Case D* in the critical case under combined bending and shear are shown in Fig 31.

As can be seen in Fig 30, when the flange width is in the range from 0.01mm – 80 mm, the interaction relation curves lie slightly above the circular curve. The interaction relation is quite similar to that of *Case B* for the lipped channel described above. The interaction is significant. As the ratio of b_2/b_1 increases further from 0.5 to 0.8, the relation curves are more higher than the circular curve, so that the interaction between bending and shear is not significant. As the ratio of b_2/b_1 increases from 0.7 to 0.8, the interaction curves get closer to the circular curve. The interaction is therefore more significant. The explanation for this fact is mainly due to interaction of the actual shear stress and uniform compression stress in the flanges. As can be seen in Fig 31, the buckling mode is similar to that of *Case C* for the lipped channel described above. The mode of buckling is distortional buckling in the flange under shear and compression. There is little or no buckling in the web.

Figure 31. Buckling Mode Shape of Lipped Section under Combined Bending and Shear for *Case D*

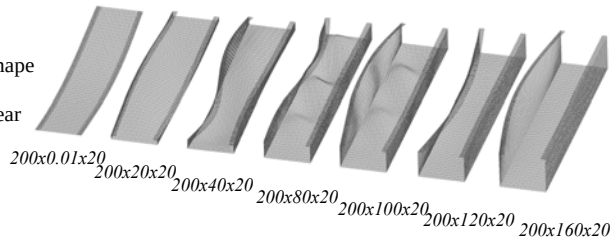

4. Conclusion

This report has outlined buckling analyses of channel section members subjected to pure shear and pure bending alone and the interaction relations under combined bending and shear. Unlipped and lipped channels were analysed by the Isoparametric Spline Finite Strip Method program. Four different shear flow distribution cases combined with pure bending were consider in this report. Two boundary were used for the analyses in this study. These boundary conditions are simply supported with and without lateral restraints along two longitudinal edges of web panel. The aspect ratio of the rectangular plate a/b_1 of 5.0 was chosen to investigate the interaction relation between bending and shear.

By varying the flange width, the analysis results show that the flanges can have a significant influence on the interaction relation between bending and shear. It is demonstrated that the twisting mode of sections with narrow flanges can lead to significant interaction under combined bending and shear. As the flange width increases, the interaction relation is proven to be less significant. The main reason is that the uniform compression stress in a very wide flange causes distortional buckling which does not appear to be significantly affected by shear stress.

5. References

Allen, H. G and Bulson, P. 1980. "Background to Buckling", *McGraw-Hill Book.*

Bleich, H. 1952. "Buckling Strength of Metal Structures", *McGraw-Hill Book Co. Inc*, New York, N.Y.

Bulson, P. S. 1970. "Stability of Flat Plates", *Chatto & Windus Ltd.,* London W.C.2.

Cheung, Y. K. 1976. "Finite Strip Method in Structural Analysis", *Pergamon Press, Inc.*, New York, N.Y.

Eccher, G. 2007. "Isoparametric spline finite strip analysis of perforated thin-walled steel structures", *PhD Thesis, The University of Sydney, University of Trento,* Australia & Italia.

Kwon, Y. B. and Hancock, G. J. 1991. "A Nonlinear Elastic Spline Finite Trip Analysis for Thin-Walled sections", *Thin-Walled Structures*, Vol. 12 1991, pp 295-319.

Lau, S. C. W. and Hancock, G. J. 1986. "Buckling of Thin Flat-Walled Structures by a Spline Finite Strip Method", *Thin-Walled Structures*, Vol. 4 1986, pp 269-294.

Lau, S. C. W. and Hancock, G. J. 1989. "Inelastic Buckling Analysis of beams, Columns and Plates using the spline finite strip method", *Thin-Walled Structures*, Vol. 7 1989, pp 213-238.

Pham, C. H. and Hancock, G. J. 2007. "Shear Buckling of Thin-Walled Channel Sections", *Research Report No R885*, School of Civil Engineering, The University of Sydney, NSW, Australia, August, 2007.

Timoshenko, S. P. and Gere, J. M. 1961. "Theory of Elastic Stability", *McGraw-Hill Book Co. Inc*, New York, N.Y.